Characterization of the Particle Emission from Ships Operating at Sea Using Unmanned Aerial Vehicles

Tommaso F. Villa[1], Reece Brown[1], E. Rohan Jayaratne[1], L. Felipe Gonzalez[2], Lidia Morawska[1], Zoran D. Ristovski[1*]

[1] International Laboratory for Air Quality and Health (ILAQH), Queensland University of Technology (QUT), 2 George St, Brisbane QLD 4000

[2] Australian Research Centre for Aerospace Automation (ARCAA), Queensland University of Technology (QUT), 2 George St, Brisbane QLD 4000

Correspondence to: Zoran D. Ristovski (z.ristovski@qut.edu.au)

Abstract. This research demonstrates the use of an unmanned aerial vehicle (UAV) to characterize the gaseous (CO_2) and particle (10 - 500 nm) emissions of a ship at sea. The field study was part of the research voyage "The Great Barrier Reef as a significant source of climatically relevant aerosol particles" on-board the RV Investigator around the Australian Great Barrier Reef. Measurements of the RV Investigator exhaust plume were carried out while the ship was operating at sea, at a steady engine load of 30%.

The UAV system was flown autonomously using several different programmed paths. These incorporated different altitudes and distances behind the ship in order to investigate the optimal position to capture the ship plume. Five flights were performed, providing a total of 27 horizontal transects perpendicular to the ship exhaust plume. Results show that the most appropriate altitude and distance to effectively capture the plume was 25 m above sea level and 20 m downwind.

Particle number emission factors (EF_{PN}) were calculated in terms of number of particles emitted (#) per weight of fuel consumed (Kg fuel). Fuel consumption was calculated using the simultaneous measurements of plume CO_2 concentration. The calculated EF_{PN} was $7.6 \pm 1.4 \times 10^{15}$ #.Kg_{fuel}^{-1}, which is in line with those reported in the literature for ship emissions ranging from 0.2×10^{16} #.Kg_{fuel}^{-1} to 6.2×10^{16} #.Kg_{fuel}^{-1}.

This UAV system successfully assessed ship emissions to derive EF_{PN} under real world conditions. This is significant as it provides a novel, inexpensive and accessible way to assess ship EF_{PN} at sea.

1.   Introduction

Shipping is the most significant contributor to international freight, with almost 80% of the worldwide merchandise trade by volume transported by ships in 2015 (UNCTAD, 2015). Emissions from this transportation mode are a significant contributor to air pollution, both locally and globally. Ships are a major pollutant source in areas surrounding harbours (Viana et al., 2014), with over 70% of emissions reaching 400 km inland (Fuglestvedt et al., 2009). In 2012 exhaust from diesel engines, the predominant source of ship power, was classified as a group 1 carcinogen by the International Agency for Research on Cancer (IARC). In 2007, pollution from ship exhaust was found to be responsible for approximately 60,000 cardiopulmonary and lung cancer deaths worldwide annually (Corbett et al., 2007a). Such emissions are also a strong climate forcing agent, contributing to global warming through the absorbance of solar and terrestrial radiation (Winnes et al., 2016;Hallquist et al., 2013a;Lack et al., 2011).

Despite these findings, emissions from shipping have consistently been subject to less regulation than those of land-based transport with ship emissions in international waters remaining one of the least regulated parts of the global transportation system (Cooper, 2001, 2005;Corbett and Koehler, 2003;Corbett and Farrell, 2002;Eyring et al., 2005;Streets et al., 1997;USEPA-OTAC, 2012). Currently, no specific restrictions for ship-emitted particulate matter (PM) exist, with the only regulated pollutants being NOx and SO_2. The International Maritime Organization (IMO) recently revised the regulation of

40 these gaseous pollutants through the Annex VI of the International Convention for the Prevention of Pollution from Ships –

41 the Marine Pollution Convention (MARPOL). The IMO expected that these regulations would lead to an indirect decrease in

42 particle number (PN) concentration due to the reduction of NOx emissions and the use of fuel with lower sulphur content [14].

43 However, it has been found that the use of some low sulphur fuels lead to increased PN concentrations at lower engine loads

44 (Anderson et al., 2015), which stresses the importance for regulation specifically addressing particulate matter (PM).

45 The majority of emitted PM is in the ultrafine size range, < 0.1 μm, which have been demonstrated to have a particularly

46 significant impact on health and the environment (WHO, 2013). However, due to the lack in regulation, ultrafine particles, in

47 terms of PN concentration, emitted from ships have remained unassessed in real world conditions. Quantifying PN

48 concentration is critical to improve our understanding of shipping's impact on health and climate (Chen et al., 2005;Cooper,

49 2001;Corbett and Farrell, 2002;Isakson et al., 2001;Williams et al., 2009;Reda et al., 2015;Mueller et al., 2015;Anderson et

50 al., 2015;Blasco et al., 2014;Ristovski et al., 2012;Corbett et al., 2007b). To achieve this, wide-scale evaluation of ship

51 emission factors (EFs) is necessary. EFs are commonly expressed as the amount of pollutant (x) emitted per unit mass of fuel

52 consumed g(x). (Kg fuel)$^{-1}$. Different methods have been used to investigate ship EFs, including laboratory test-bench studies,

53 on-board measurements, and measurement of ship emission plumes.

54 Test-bench studies (Reda et al., 2015;Mueller et al., 2015;Anderson et al., 2015;Petzold et al., 2010;Petzold et al., 2008;Kasper

55 et al., 2007) have been used to characterize emissions from different engines at various loads in laboratory conditions.

56 However, engine performance and emissions have been shown to be different in real world operations when compared to

57 laboratory studies. This calls for measurements of ship emissions in-situ to collect reliable data for EF calculations (Blasco et

58 al., 2014;Murphy et al., 2009;Agrawal et al., 2008). To date, only a few studies have been undertaken on-board ships to

59 calculate real emission factors (Juwono et al., 2013;Hallquist et al., 2013b). This is attributed to the prohibitive costs and time

60 commitments of setting up and maintaining on-board measurement equipment on commercial ships. Airborne ship plume

61 measurements (Westerlund et al., 2015;Schreier et al., 2015;Pirjola et al., 2014;Cappa et al., 2014;Beecken et al., 2014;Balzani

62 Lööv et al., 2014;Berg et al., 2012;Lack et al., 2009;Lack et al., 2008;Sinha et al., 2003) offer an alternative method of in-situ

63 measurements without requiring on-board monitoring stations. In the past the deployment cost of these systems, and the risks

64 associated with manned aircrafts have limited their feasibility. However, this has recently changed with the rapid advances

65 being made in commercially available Unmanned Aerial Vehicle (UAV) technology.

66 Hexacopter UAVs have seen a wide scale increase in industry and research applications due to their ease of use and

67 comparatively low cost (Malaver Rojas et al., 2015;Gonzalez et al., 2011;Brady et al., 2016). Used in conjunction with air

68 monitoring equipment, these systems provide, for the first time, the ability to perform relatively simplistic and cost-effective

69 airborne measurements of ship emissions. However, to date no studies have reported the use of a UAV system capable of

70 collecting data to calculate the EF of PN concentration for ships at sea.

71 This research utilized a customized hexacopter UAV carrying instruments for PN concentration and CO_2 measurements to

72 derive EF_{PN}. The UAV system was deployed from the RV Investigator research vessel while at sea. Autonomous measurements

73 of the RV investigators exhaust plume were taken over several flights at various altitudes and distances from the ship. Data

74 collected was used to optimize the sampling flight path and successfully quantify the RV investigators EF for PN concentration.

75 **2.   Methodology and Measurement system**

76 Measurements were conducted as part of the research voyage "The Great Barrier Reef as a significant source of climatically

77 relevant aerosol particles" aboard the RV Investigator research vessel over a two day period of the 13 and 14 October 2016

78 (day 1 and day 2). Measurements of PN and CO_2 concentration emitted by the RV Investigator were taken using a PN and CO_2

79 monitor mounted on a customized DJI EVO S800 hexacopter UAV (DJI, 2014).

2.1. The RV Investigator and the voyage

The RV Investigator is an ocean research vessel configured to enable a wide range of atmospheric, biological, goescience and oceanographic research. The vessel is 94 m long, has a gross weight of 6,082 tons, a fuel capacity of 700 tons of ultra-low sulphur diesel fuel. It is powered by three 9 cylinder 3000 kW MaK diesel engines, each coupled to a 690V AC Generator. Ship propulsion is achieved using two 2600 kW L3 AC reversible propulsion motors powered by these generators. The RV Investigator can host up to 30 crew members and 35 researchers for a maximum voyage period of 60 days with a maximum cruising speed of 12 knots.

A suite of instrumentation for atmospheric research is available on the RV Investigator. This includes a radar system capable of collecting weather information within a 150 km radius of the vessel, and instruments measuring: sunlight parameters; aerosol composition, particle concentration and size distributions; cloud condensation nuclei; gas concentrations; and various other components of the atmosphere. These instruments are housed inside two dedicated on-board laboratories for aerosol and for atmospheric chemistry research. An atmospheric aerosol sample is continuously drawn into the laboratories for analysis through a specialized inlet fitted to the foremast of the ship. Of particular interest to this study, the ship contains a PICARRO (PICARRO Inc., Santa Clara, California, USA) G2401 analyser (Inc., 2017) that continuously measures CO_2, CO, H_2O and CH_4. It has an operation range between 0-1000 ppm and a parts-per-billion sensitivity (ppb) for CO_2.

The two day UAV measurement study was possible as part of the RV Investigator voyage "The Great Barrier Reef as a significant source of climatically relevant aerosol particles", which started in Brisbane on the 28th of September 2016. The ship was used as both: a floating platform to allow launch and recovery of the UAV system; and as the source of an exhaust plume measured by the UAV system for EF calculation. During a several day stationary period on the Great Barrier Reef off the coast of Australia, it was possible to measure the ship plume under stable real world conditions over two consecutive days. One of the three ship engines was maintained at a steady engine load of 25 – 30 % of the maximum engine power during all measurements.

2.2. UAV system

Measurements of PN and CO_2 concentrations in the ship plume were performed using two commercial sensors mounted on-board a hexacopter UAV. The UAV used (Figure 1) is a composite material S800 EVO manufactured by DJI (DJI, 2014). The UAV is 800 mm wide and 320 mm in height, with an unloaded weight of 3.7 kg. Minimum and maximum take-off weights are 6.7 kg and 8 kg, respectively. The UAV contains a 16000 mAh LiPo 6 cell battery, which provides a hover time of approximately 20 min when operating at minimum take-off weight. The telemetry range of the UAV is 2 km, which was adequate to cover the desired sampling area (See Figure 2).

The payload consisted of a PN concentration and a CO_2 monitor mounted on-board underneath the UAV. Careful placement of the payload was required to prevent flight issues caused by an altered centre of gravity. Also included was a carbon fibre rod, which extended outward horizontally from the UAV. The sampling lines for the monitors were attached to the end of this rod to ensure that measurements were not affected by the downwash of the UAV rotors. The total weight of the payload was (1.2 kg), which allowed the UAV system to fly for 12-15 min before landing at the home point (A) (See Figure 2).

The S800 was used in conjunction with the DJI Wookong autopilot. The software provides an intuitive and easy to use interface where autonomous flight paths can be planned, saved, and uploaded into the UAV. In addition to this, the ground station allows for continuous, real-time monitoring of the status of the UAV during operation; which includes its longitude, latitude, altitude, waypoint tolerance and airspeed.

The DJI S800 was chosen for this study because it is designed to operate under the 20 kg all up weight (AUW) class of UAV. This reduces operational costs and avoid subjection to the tighter regulations of larger platforms. Small UAV cannot be operated above any person, or closer than 30 m of populated areas, houses and people. Furthermore, current Civil Aviation Safety Australia (CASA) regulations restrict the use of small UAV (2 and 20 kg) to visual line-of-sight daylight operation,

with a maximum altitude of approximately 120 m and within a radius of 3 nmi of an airport. UAVs in this category are not permitted for research unless the research institution has been granted a permit exception. These exceptions can be granted if the institution in question has or collaborates with an UAV operation team who must have: an experienced UAV pilot who is also radio controller specialist; a license for commercial UAV operation; and appropriate liability insurance (NPRM 1309OS - Remotely Piloted Aircraft Systems). Queensland University of Technology (QUT) has an unmanned operator certificate and four pilots who have UAV controller licenses.

2.2.1.   Instrumentation

2.2.1.1.   Instrumentation for PN concentration

This study measured PN concentration using a Mini Diffusion Size Classifier (DISCmini), developed by the University of Applied Sciences, Windisch, Switzerland (Fierz et al., 2008). The DISCmini is a portable monitor used to measure concentration of particles in the 10-500 nm diameter size range, with a time resolution of up to 1s (1 Hz). It can measure PN concentrations between 10^3 and 10^6 N/cm^3. Measurement accuracy is dependent upon the particle shape, size distribution, and number concentration. The advantages of using the DISCmini are its relatively small dimensions (180 x 90 x 40 mm), low weight (640 g, 780 g with the sampling probe, Figure 1) and long battery life of up to 8 hrs. These characteristics allow it to be easily integrated on the UAV.

2.2.1.2.   Instrumentation for CO2 concentration measurements

A TSI (TSI, Shoreview, Minnesota, United States) IAQ-calc 7545 model was chosen to measure CO_2 concentrations. Its sensor is based on a dual-wavelength NDIR (non-dispersive infrared) with a sensitivity range between 0 to 5,000 ppm and an accuracy of ± 3.0% of reading or ± 50 ppm (whichever is greater). The measurement resolution is 1 ppm with a maximum time resolution of 1s. Similar to the DISCmini, the advantages of using the IAQ-calc are: its small dimensions (178 x 84 x 44 mm); low weight (270 g, with batteries, significantly lower than the DISCmini), and a battery life of 10 hours.

The readings of the IAQ-clac for CO_2 were compared with those measured by the on-board PICARRO G2401 analyser.

Both the DISCmini and the IAQ-calc were tested and calibrated in the on-board laboratory using ambient aerosol measurements at sea prior to the commencement of the measurements (Figure S2 in the Supplementary Material). All data were logged with a 1 s time interval.
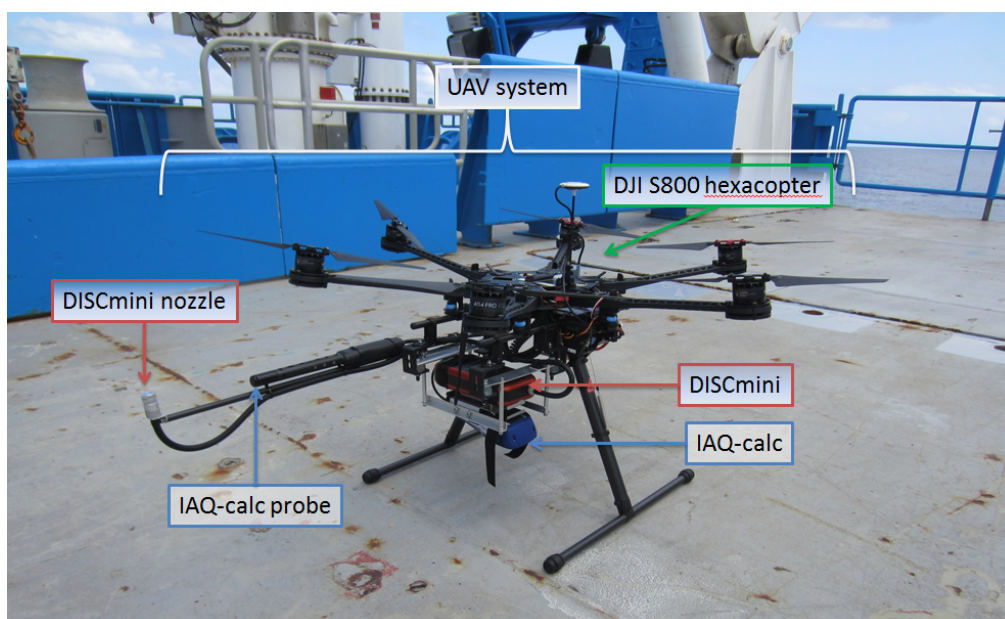
Figure 1. The UAV system with the on-board instrumentation: the DISCmini and the IAQ-calc.

2.3. Meteorological data

Meteorological data (including air temperature, relative humidity, atmospheric pressure, wind speed and direction) were recorded by the RV Investigators on-board instrumentation during the entire voyage with a 60 s time interval, 24/h a day.

2.4. Study design

During the two measurement days of this study, the vessel was heading into the wind whilst idling the UAV missions at sea. This positioning caused the exhaust plume to extend downwind, directly behind the ship. The UAV system was launched off the back deck, autonomously sampling at varying altitudes and distances into the downwind plume. Flight speed of the UAV was 1.5 m/s, the minimum for the S800.

Day 1 was used to optimise the study design, focusing on finding the flight path most suitable to capture the ship plume. Figure 2 shows the programmed flight path, which consisted of a continuous flight beginning at a distance (D) and from an altitude (H) above the surface. Point A, located on the back deck of the RV Investigator, represents the 'home point'. In UAV terminology this refers to the position where the UAV system takes off and lands. The UAV system was programmed to move horizontally by a distance (2d), perpendicular to the ship, then climb vertically for 10 m (h) before flying in the opposite horizontal direction for the same distance (2d). The UAV was then programmed to climb another 10 m (h) before repeating this pattern until the UAV reached an altitude of 65 m above the ocean. During day 1, the UAV system followed three different flight paths, each one with both a different distance D behind the ship (20, 50 and 100 m), and a different horizontal distance 2d (50, 100 and 150 m).

The optimised flight path for day 2 started 20 m behind the ship and 25 m above the surface, with no altitude variation. The UAV path was limited to a continuous horizontal flight of 50 m (2d) at steady speed of 2 m s^{-1}. This path and flying speed allowed up to 4 horizontal transects to capture the ship plume.
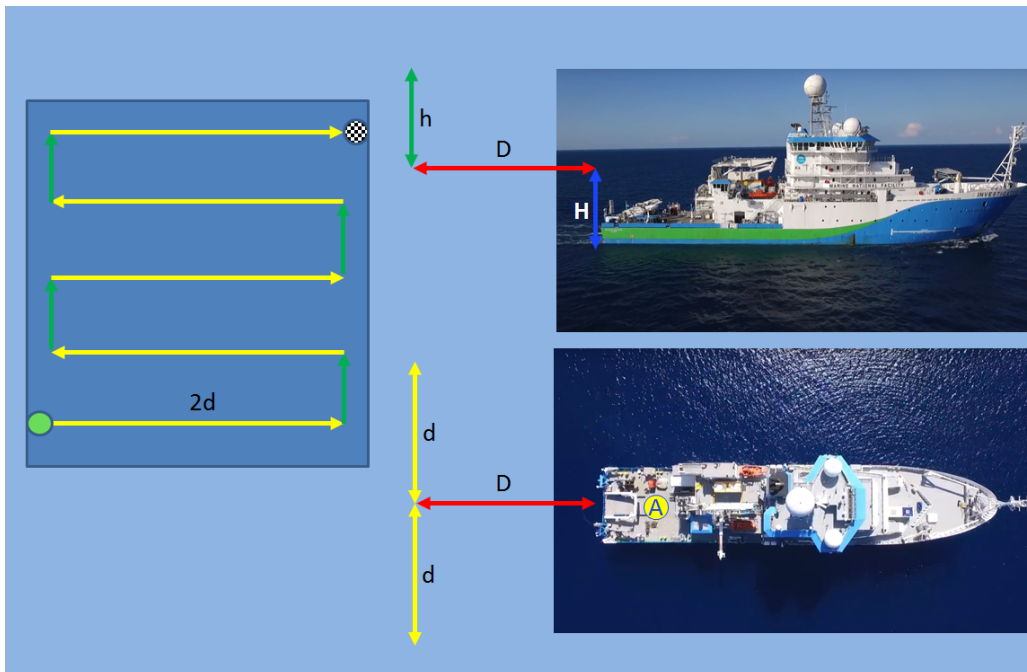
Figure 2. Flight path used to capture the plume: H - height from the ocean, D – distance behind the ship to the flight beginning point, h – rising altitude after the horizontal transect, 2d – full length of the horizontal transect

2.5. Experimental procedure

The UAV can fly either manually or autonomously. As a safety precaution, every take-off and landing was performed using the manual flight mode. Once in the air, the UAV was switched to autonomous flight mode, allowing the platform to follow the pre-programmed flight path discussed in the previous section. The flight path consisted of waypoints, which are three-

177 dimensional GPS points that dictate the position of the UAV along the fight path. The waypoints and flight plans for each

178 flight were programmed using the aforementioned DJI Wookong ground station software. The DISCmini and the IAQ-calc

179 were fitted on the underside of the UAV at the beginning of each measuring day. Five flights were performed across the two

180 measurement days, providing a total of 27 horizontal transects perpendicular to the ship's exhaust plume.

181 **2.6.   Emission factors**

182 The calculation of an emission factor for particle number concentration (EF_{PN}) from the collected ship plume measurements

183 was performed using Eq. (1). This method has previously been used for ship (Westerlund et al., 2015), road vehicle (Hak et

184 al., 2009) and aircraft (Mazaheri et al., 2009) emissions. The measured values of PN concentration were related to the amount

185 of fuel consumed by the engine in question through the use of the simultaneous measurements of CO_2 concentration taken by

186 the UAV. This was achieved by using a published value for a ship emission factor of CO_2 (EF_{gas}) of 3.2 Kg CO_2 (Kg fuel)$^{-1}$

187 (Hallquist et al., 2013b;Hobbs et al., 2000) .

188 Eq.(1).

189 $$EF_{PN} = \frac{\Delta PN}{\Delta gas} \text{ x } EF_{gas} \tag{1}$$

190 The ΔPN and Δgas in Eq. (1) represent the maximum particle concentration change above background in the measured

191 particle number and CO_2 concentrations, respectively. The DISCmini measurements were corrected against a reference CPC.

192 For each transect data series of PNC and CO_2, the averaged background concentration were subtracted from the peak data

193 corresponding to measurements inside the plume. The corrected peak data series were then fit with a Gaussian curve using the

194 inbuilt Matlab curve fitting application. The least absolute residuals (LAR) condition was used as this most closely fits the

195 curve to the highest magnitude data points in the series. The maximum peak height of the fitted Gaussian curves were used as

196 ΔPNC and ΔCO_2 in the calculation of emission factors for each transect.

197 **3.   Results and Discussion**

198 **3.1.   Meteorological and Investigator data**

199 Wind conditions were very stable during both day 1 and day 2, following one main pattern for the entire flight time. The wind

200 speed ranged from 3 - 13 m s-1. The wind direction was predominantly from the NE during day 1 and ESE during day 2. The

201 wind rose graphs in Figure 3a and 3b illustrate the wind data recorded with the on-board weather instrumentation during all

202 horizontal transects flown during day 1 and 2 respectively. The prevalent wind direction was ESE, which corresponded to the

203 heading of the RV Investigator (indicated by the rose triangle). The wind direction changed occasionally to E during the flight,

204 causing the UAV to fail to capture the RV Investigator plume during some transects. As a result, 2 of the 8 horizontal transects

205 collected on day 2 were excluded from the analysis.

206

207
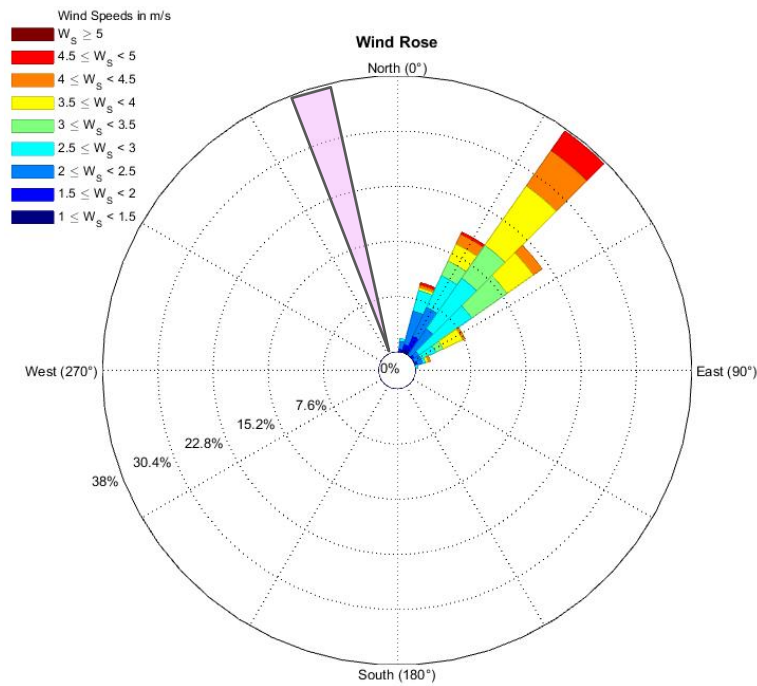
Figure 3a – Wind rose showing wind speed and direction during day 1. Rose triangle shows RV Investigator direction during the measurements.

210

211
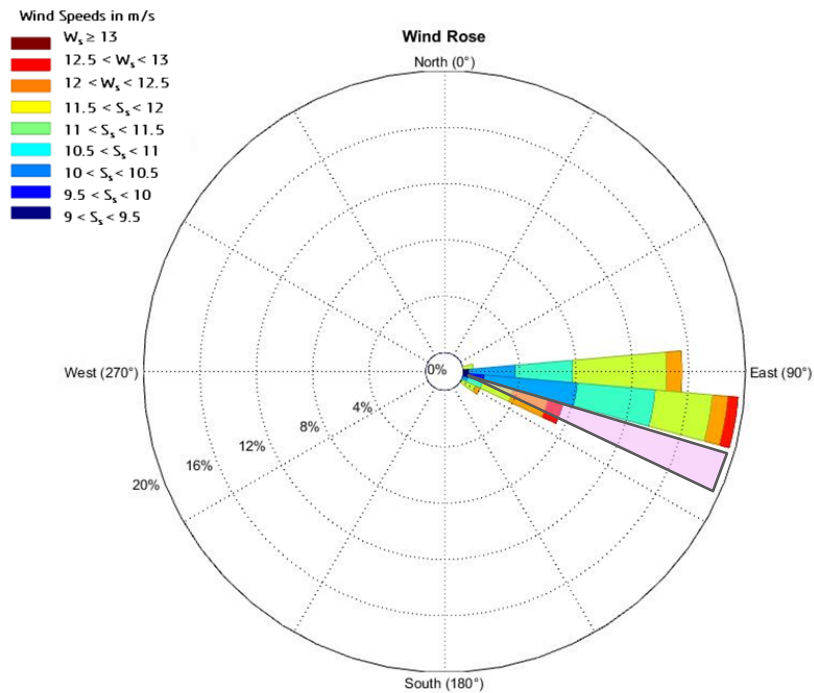
Figure 3b – Wind rose showing wind speed and direction during day 2 optimized flight. Rose triangle shows RV Investigator direction during the measurements.

3.2. UAV system horizontal transects inside and outside the plume

The UAV system acquired data for a total of 27 horizontal transects for day 1 and day 2. Data were collected at altitudes between 25 m and 65 m above the water surface. During day 1 the plume was captured once when the UAV was at 25 m

217 altitude and 20 m downwind of the ship; and again at both 25 and 35 m altitude 100 m downwind of the ship. These

218 observations lead to the optimized flight used on day 2, which started downwind at 25 m above the surface and 20 m behind

219 the ship. On day 2 the UAV system successfully captured the plume during 6 of the 8 transects performed. Across the two

220 days this lead to a total of 9 transects that captured the plume and which have been considered for discussion, shown in Table

221 1.

222

Measuring day	Altitude	Distance behind the Investigator	Number of transects
Day 1	25 m	20 m	1
*Day 1	25 m	100 m	1
Day 1	35 m	100 m	1
Day 2	25 m	20 m	6

223

224 **Table 1 – Specifications of the transects considered for the data analysis. The (*) indicates the transect of Day 1 of which PN**

225 **concentration and CO_2 profiles are presented in Figure 4.**

226

227 Figure 4 shows the PN concentration and CO_2 profiles, collected during two (a; b) transects on day 2, and (c) during one

228 transect of day 1 (Spec. in Table 1, Day1*).

229 The PN concentration profiles for the (a) and (b) transects in Figure 4 show that the concentration varied by five orders of

230 magnitude between the outside and inside the plume, while the CO_2 profiles show an increase up to 140 ppm above the

231 background.

232 The profiles in (c) show that the PN concentration was four orders of magnitude greater inside the plume at 100 m behind the

233 ship and that the CO_2 concentration was up to 70 ppm higher inside the plume.
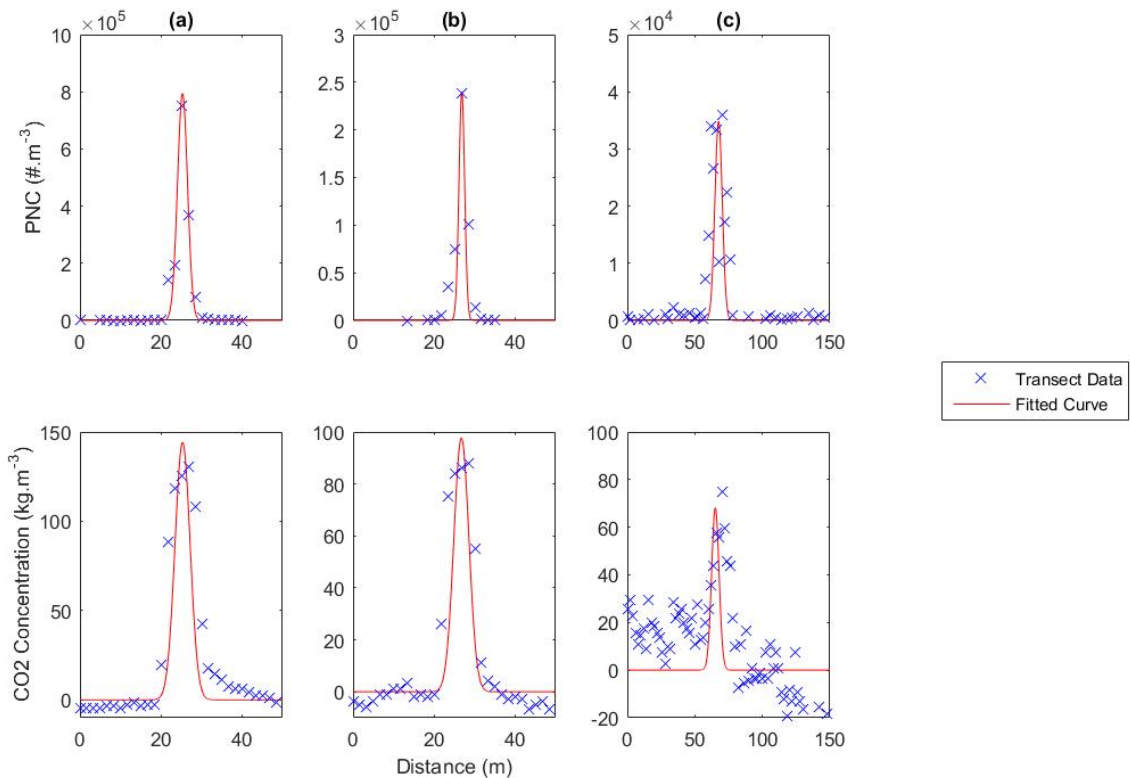
234

235 **Figure 4 – (a) and (b) show the measured PN and CO$_2$ concentration profiles and fitted Gaussian curves for two different transects**

236 **20 m behind the ship 25 m above the surface during day 2. (c) shows the PN and CO$_2$ concentration profiles and fitted Gaussian**

237 **curves collected during flight 3 of day 1 at 100 m behind the ship, 25 m above the surface.**

238

239 Figure 4 (a) and (b) both show transects at 25 m altitude and 20 m behind the ship. Both the PN concentration and CO$_2$

240 measurements show clear, single peaks as the UAV crosses the plume. As a consequence, these transects show a good fit with

241 the corresponding Gaussian distribution curves with R^2 values of above 0.9 for both PNC and CO$_2$. In contrast Figure 4 (c)

242 shows substantially less defined, wider peaks with lower pollutant concentrations. This is attributed to a difference in flight

243 paths, with Figure 4 (c) representing data from a transect 100 m behind the ship. The additional time between emission and

244 sampling has allowed the plume to broaden, become less homogenous, and take on a skewed cross-section. This results in a

245 significantly lower R^2 value for the fitted Gaussian curves, with a value of 0.4998 for the CO$_2$ data in this transect. Therefore,

246 whilst the 100 m transect does provide more data points inside the plume, the randomized variations inside the plume lead to

247 less accurate calculations of emission factors.

248 Of further note in Figure 4, the maximum PN concentrations measured in (a) (7.5×10^5 #.cm^{-3}) is approximately three times

249 greater than those in (b) (2.4×10^5 #.cm^{-3}) and the CO$_2$ concentrations in (a) are 43 ppm greater than (b). The transect flight plan

250 and ship engine load remained constant throughout these measurements. The variations between (a) and (b) are attributed to

251 several factors which reduce the effectiveness of the UAV transect for capturing the plume. Slight changes in ambient

252 conditions such as temperature, wind direction and intensity will alter the path of the plume as it moves away from the ship.

253 The UAVs automated flight path cannot account for these variations. Therefore, the degree to which the UAV enters the plume,

254 and thus the concentrations it measures, will be different on each transect. Both CO$_2$ and PN concentration measurements will

255 be similarly affected by this variance. However, differences in instrument response rates in conjunction with these variances

256 will be one of the major contributors to variations in calculated emission factors.

257 **3.3.   PN Emission Factors**

258 Table 2 shows the distance and altitude of each transect, the R^2 values of the fitted Gaussian curves for PNC and CO$_2$ data, the

259 calculated values of ΔPNC and ΔCO$_2$, and the calculated EF$_{PN}$.

Day	Dist/Alt (m)	R^2_{PNC}	R^2_{CO2}	ΔPNC (#.m^{-3})	ΔCO$_2$ (kg.m^{-3})	EF$_{PN}$ (#.kg$_{fuel}^{-1}$)
1	100/25	0.9586	0.4998	5.05E+11	9.35E-05	1.73E+16
	100/35	0.4767	0.8967	4.8E+10	1.34E-04	1.15E+15
	20/25	0.9856	0.8915	1.09E+11	7.74E-05	4.52E+15
2	20/25	0.9842	0.9518	1.06E+12	2.83E-04	1.20E+16
	20/25	0.9852	0.8838	3.3E+11	1.92E-04	5.51E+15
	20/25	0.9489	0.9246	1.78E+11	1.11E-04	5.16E+15
	20/25	0.9721	0.8965	3.6E+11	2.23E-04	5.18E+15
	20/25	0.9508	0.8473	1.47E+11	1.31E-04	3.59E+15
	20/25	0.8517	0.6743	1.01E+11	9.68E-05	3.32E+15

261 **Table 2 – Transect flight days and details, R^2 values for the Gaussian curve fits to both PNC and CO$_2$ data, ΔPNC and ΔCO_2**

262 **concentration emission/rate of the RV Investigator, and calculated Emission Factors for PN.**

263

264 The calculated EF$_{PN}$ values for the RV Investigator ranged from 1.15×10^{15} to 1.73×10^{16} #.Kg$_{fuel}^{-1}$. The two 100 m transects

265 provided the worst Gaussian fits as well as the highest and lowest calculated emission factors. This indicates that it is important

266 to filter out transects with data which does not fit the expected Gaussian distribution suitably as they can generate significant

267 error. To this end, the 100 m transects were excluded from further analysis. ΔPNC and ΔCO₂ values for remaining transects
268 were plotted against each other as shown in Figure 5.

269
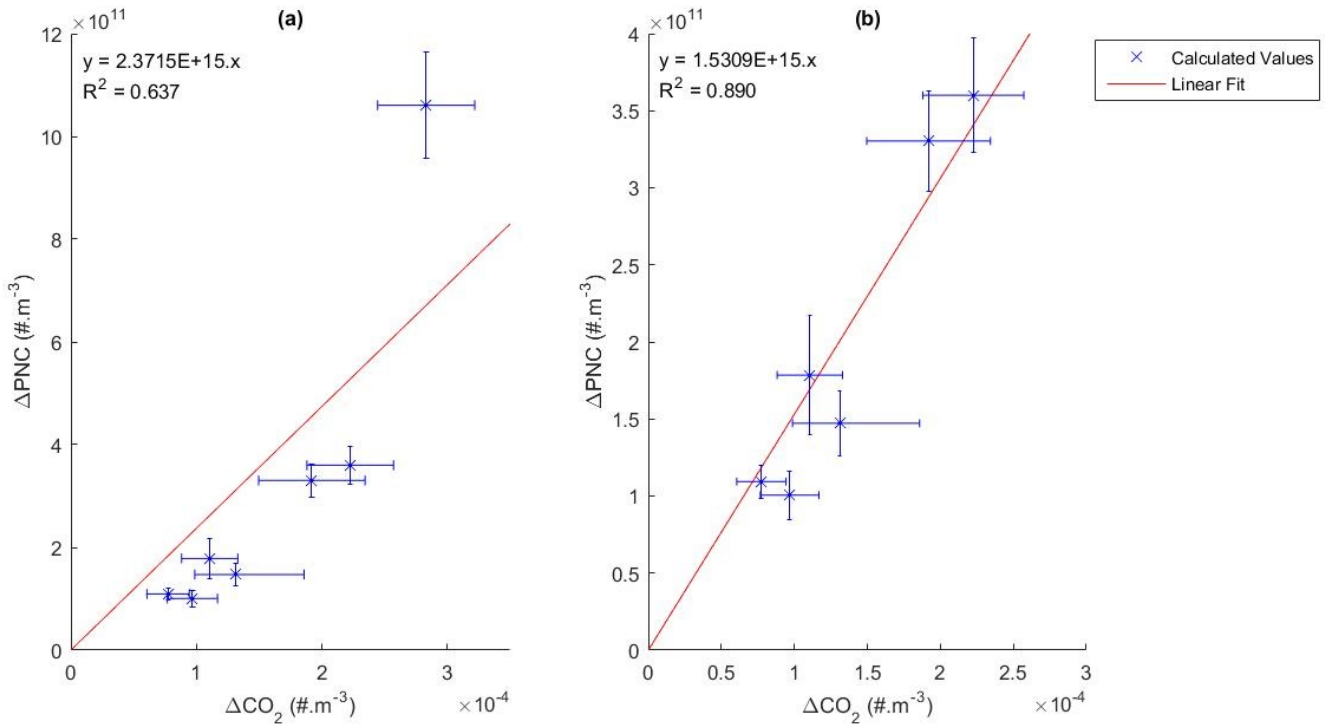
270 **Figure 5 –(a) ΔPNC against ΔCO₂ with 95% confidence interval for the six transects considered for the data analysis. (b) ΔPNC**
271 **against ΔCO₂ with 95% confidence interval with the removal of the outlier transect from the first flight of day 2**

272

273 Figure 5 (a) and (b) show the plots of the remaining transects ΔPNC against ΔCO₂ with and without the values of the first
274 flight of day 2. This transect represents a clear outlier in the linear trend, with the R^2 value of the linear fit increasing from
275 0.637 to 0.890 with its exclusion. Furthermore, whilst the linear fit falls within the confidence interval of only one point in (a),
276 it falls within all data points confidence intervals in (b). This occurs despite both R^2 values for the fitted Gaussians of this
277 transect being very high (R^2_{PNC} = 0.9842, R^2_{CO2} = 0.9518). This highlights a limitation with this methodology which can be
278 best observed in the difference between Figure 4 (a) and (b). The combination of UAV velocity, sampling rate and response
279 time of the DISCmini results in the PNC transect data having only one data point defining the peak height of the transect.
280 Relying on a single sample point leads to the potential for random instrumentation effects heavily biasing results in a way
281 which does not strongly impact the R^2 values of Gaussian fits used to identify successful transects. Therefore, it is unclear
282 whether this is a variation in the ship emissions or an instrumentation error.

283 The slope and standard error of the linear fit for Figure 4 (a) was input unto Equation 1 to calculate an overall emission factor
284 of 7.6 ± 1.4 x 10^{15} #.kg$_{fuel}^{-1}$ As presented in Table 3, this value is comparable with those reported in the literature for cruise
285 and cargo ship plumes; which range from 0.2 x 10^{16} to 6.2 x 10^{16} **#.Kg$_{fuel}^{-1}$** {, #45;Alföldy, 2013 #52;Beecken, 2014
286 #34;Jonsson, 2011 #53;Juwono, 2013 #29;Lack, 2011 #7;Lack, 2009 #37;Pirjola, 2014 #32;Sinha, 2003 #39;Westerlund, 2015
287 #30}

288

Reference	Platform	EFPN $(\#.\text{kg}_{fuel}^{-1})$	Number of ships	Location
This Study	UAV	$7.6 \pm 1.4 \times 10^{15}$	1	Open Water
Westerlund et al. (2015)	Land Based	$2.35 \pm 0.20 \times 10^{16}$	154	Harbor, Ship Channel
Beecken et al. (2014)	Airborne	$1.8 \pm 1.3 \times 10^{16}$	174	Open Water
Pirjola et al. (2014)	Land Based	0.32×10^{16}	11	Harbor, Ship Channel
Alföldy et al (2013)	Land Based	0.8×10^{16}	497	Harbor
Juwono et al. (2012)	On Board	0.22×10^{16}	2	Harbor, Ship Channel
Jonsson et al. (2011)	Land Based	$2.55 \pm 0.11 \times 10^{16}$	734	Harbor
Lack et al. (2009)	Ship	$0.71 \pm 0.55 \times 10^{16}$ (>13nm)* $1.27 \pm 0.95 \times 10^{16}$ (>5nm)**	172 165	Open Water, Shipping Channel
Lack et al. (2011)	Airborne	$1.0 \pm 0.2 \times 10^{16}$	1	Open Water
Sinha et al. (2003)	Airborne	$6.2 \pm 0.6 \times 10^{16}$	2	Open Water

Table 3 – Comparison of the Emission Factor for the RV Investigator found in this study with other relevant values found in literature. * PN$_{EF}$ for particles above 13nm. ** PN$_{EF}$ for particles above 5nm.

The calculated EF_{PN} for the Investigator was lower compared to those reported by Beecken at al. (Beecken et al., 2014) for passenger ships while accelerating ($0.91 \pm 0.18 \times 10^{16}$ $\#.\text{Kg}_{fuel}^{-1}$). However, the RV Investigator measurements were undertaken whilst its engine was under 30% load. Accelerating ships will typically be under higher engine loads and hence have a correspondingly higher EF_{PN} (Westerlund et al., 2015), which explains part of this discrepancy. Furthermore, the RV Investigator has high efficiency engines and utilizes ultra-low sulphur diesel fuel. Studies have shown that similar diesel engines burning fuel of this type have lower EF$_{PN}$ than the same engine with higher sulphur content diesel (Chu-Van et al., 2017). Similar quality fuels used in the ground transport industry have yielded similar values of EF$_{PN}$, ranging from 4.8×10^{14} (25% engine load) to 7.2 (100% engine load) $\times 10^{15}$ $\#.\text{Kg}_{fuel}^{-1}$ (Jayaratne et al., 2009).

3.4. Instrumentation Limitations

Lightweight UAVs present an opportunity to achieve aerial measurements at significantly less upfront and operational costs than fixed wing and manned aerial vehicles. Lightweight UAVs can be deployed faster with limited or no required launch and landing area compared to their manned and fixed wing counterparts. Yet, their primary disadvantage, particularly in this application, is a severely limited payload weight. To overcome this limitation, this project used the lightweight and portable DICSmini and IAQ-calc sensors. However, these instruments have lower sensitivities and greater uncertainties when compared to a high accuracy CPC and CO_2 monitor for measurements, which can influence results.

The DISCmini has a manufacturer listed measurement cut-off size of 10 nm. A previous study listed in Table 3 (Lack, Corbett et al. 2009) shows that the cut-off size of instruments used to measure PNC is directly linked to the value of EF$_{PN}$, with the measured EF$_{PN}$ doubling when the cut-off size is changed from 13 nm to 5 nm due to the large number of particles in this size range. This may have been another contributing factor to the EFPN measured in this study being in the lower end of measured values in literature.

The two 100m transects were not accounted for in the final calculation of EF$_{PN}$ due to their poor Gaussian curve fits. Whilst this has been attributed to the skewing of the plume at this distance, the limitations of the instrumentation could also have contributed. The lower concentrations of CO_2 at this distance result in the difference above background inside the plume being the same order of magnitude as the manufacturer specified error margin. Hence, the variability in the plume either side of the central peak as shown in figure 4 (c) could be due in part to instrumentation error.

317 Calibrations of sensors in this study were performed by comparison with reference instruments for ambient measurements at
318 sea. Ideally, calibration should be performed with in-plume measurements, however it was not possible to access the plume
319 with reference instrumentation on board the ship. Whilst this study provides a successful proof of concept with consistent
320 results over multiple days and flights, a validation study is needed. This should include independent measurements of EF_{PN}
321 using other established methodologies to ascertain more precise correction factors and uncertainties.

322 **4.   Summary and conclusion**

323 The UAV system used in this study successfully measured PN and CO_2 concentrations from the exhaust plume of the RV
324 Investigator whilst operating at sea. Several different flight paths were tested and an optimal transect flying perpendicular to
325 the plume at a distance of 20 meters from the ship was adopted. The EF_{PN} calculated for the RV investigator $7.6 \pm 1.4 \times 10^{15}$
326 $\#.kg_{fuel}^{-1}$ at a constant 30% engine load. This EF_{PN} was in agreement with values reported in literature, indicating this novel
327 UAV system has potential for EF_{PN} quantification pending further evaluation.

328 In comparison with other methods, the UAV system presented provides a cost effective and accessible solution for the rapid
329 measurement and quantification of ship EF_{PN}s. Its ability for deployment both in harbour and at sea, coupled with the possibility
330 of altering its flight path to account for variances in wind conditions; gives this UAV system a distinct advantage over ground
331 based and manned aerial vehicles. Furthermore, the UAV can sample considerably closer to the plume emission source than
332 other methodologies, providing higher concentration measurements for the calculation of EF_{PN}.

333 Whilst further validation is necessary, results present here indicate that this UAV system has the potential to be used a low
334 cost tool for quantification of ultrafine particle emission factors from commercial shipping. This is critical to improve our
335 understanding of shipping's impact on climate and health.

336 **4.1.   Recommendations**

337 The potential of this UAV system extend far beyond what is described here. This study is intended as both: a proof of concept;
338 and to provide useful information both for the future of this project, as well as any other UAV sampling systems being
339 developed. The most significant improvement to the method described would be the use a UAV with a lower minimum
340 airspeed. This would allow for more data points per transect and would minimize the impact potential outliers in
341 instrumentation data. Other related improvements to this include: the use of different sensors with higher response rates; and
342 additional flightpath investigations to find an optimal transect distance which provides the broadest plume cross-section,
343 without the plume becoming distorted and impacting accuracy.
344 Further optimization of the transect approach is also possible. After location of the plume the system could be set to make
345 several repeat passes across the plume in rapid succession to increase the sample size. Another alternative would involve the
346 UAV hovering inside the plume over a period of time collecting a continuous series of measurements from the centre of the
347 plume. These methods would both require real time sensor feedback to the UAV pilot and potentially adaptive autonomous
348 controls to achieve a suitable result. This methodology could also be expanded to measure other important ship emission
349 factors, including NO_X and volatile organic compounds (VOCs).

350 **Acknowledgements**

351 The authors would like to acknowledge the ARCAA Operations Team (Dirk Lessner, Gavin Broadbent) who operated the
352 Unmanned Aerial Vehicle (S800). This research was supported by the Australian Research Council Discovery Grant
353 DP150101649 and the Marine National Facility. The authors would like to thank the Captain and the crew of the RV

354 Investigator as well as the on board MNF support staff as without their support and effort this research would not have been

355 possible.

356 **Reference**

357 NPRM 1309OS - Remotely Piloted Aircraft Systems: https://www.casa.gov.au/standard-page/nprm-1309os-remotely-piloted-aircraft-
358 systems?WCMS%3ASTANDARD%3A%3Apc=PC_102028.
359 Agrawal, H., Malloy, Q. G. J., Welch, W. A., Wayne Miller, J., and Cocker Iii, D. R.: In-use gaseous and particulate matter emissions from
360 a modern ocean going container vessel, Atmospheric Environment, 42, 5504-5510, http://dx.doi.org/10.1016/j.atmosenv.2008.02.053, 2008.
361 Anderson, M., Salo, K., Hallquist, Å. M., and Fridell, E.: Characterization of particles from a marine engine operating at low loads,
362 Atmospheric Environment, 101, 65-71, http://dx.doi.org/10.1016/j.atmosenv.2014.11.009, 2015.
363 Balzani Lööv, J. M., Alfoldy, B., Gast, L. F. L., Hjorth, J., Lagler, F., Mellqvist, J., Beecken, J., Berg, N., Duyzer, J., Westrate, H., Swart,
364 D. P. J., Berkhout, A. J. C., Jalkanen, J. P., Prata, A. J., Van Der Hoff, G. R., and Borowiak, A.: Field test of available methods to measure
365 remotely SOx and NOx emissions from ships, Atmospheric Measurement Techniques, 7, 2597-2613, http://dx.doi.org/10.5194/amt-7-2597-
366 2014, 2014.
367 Beecken, J., Mellqvist, J., Salo, K., Ekholm, J., and Jalkanen, J. P.: Airborne emission measurements of SO_2 , NO_X and particles from
368 individual ships using a sniffer technique, Atmospheric Measurement Techniques, 7, 1957-1968, http://dx.doi.org/10.5194/amt-7-1957-
369 2014, 2014.
370 Berg, N., Mellqvist, J., Jalkanen, J. P., and Balzani, J.: Ship emissions of SO 2 and NO 2: DOAS measurements from airborne platforms,
371 Atmospheric Measurement Techniques, 5, 1085-1098, http://dx.doi.org/10.5194/amt-5-1085-2012, 2012.
372 Blasco, J., Duran-Grados, V., Hampel, M., and Moreno-Gutierrez, J.: Towards an integrated environmental risk assessment of emissions
373 from ships' propulsion systems, Environment international, 66, 44-47, http://dx.doi.org/10.1016/j.envint.2014.01.014, 2014.
374 Brady, J. M., Stokes, M. D., Bonnardel, J., and Bertram, T. H.: Characterization of a Quadrotor Unmanned Aircraft System for Aerosol-
375 Particle-Concentration Measurements, Environmental Science & Technology, 50, 1376-1383, 10.1021/acs.est.5b05320, 2016.
376 Cappa, C. D., Williams, E. J., Lack, D. A., Buffaloe, G. M., Coffman, D., Hayden, K. L., Herndon, S. C., Lerner, B. M., Li, S. M., Massoli,
377 P., McLaren, R., Nuaaman, I., Onasch, T. B., and Quinn, P. K.: A case study into the measurement of ship emissions from plume intercepts
378 of the NOAA ship Miller Freeman, Atmos. Chem. Phys., 14, 1337-1352, http://dx.doi.org/10.5194/acp-14-1337-2014, 2014.
379 Chen, G., Huey, L. G., Trainer, M., Nicks, D., Corbett, J., Ryerson, T., Parrish, D., Neuman, J. A., Nowak, J., Tanner, D., Holloway, J.,
380 Brock, C., Crawford, J., Olson, J. R., Sullivan, A., Weber, R., Schauffler, S., Donnelly, S., Atlas, E., Roberts, J., Flocke, F., Hübler, G., and
381 Fehsenfeld, F.: An investigation of the chemistry of ship emission plumes during ITCT 2002, Journal of Geophysical Research:
382 Atmospheres, 110, D10S90, 10.1029/2004JD005236, 2005.
383 Chu-Van, T., Ristovski, Z., Pourkhesalian, A. M., Rainey, T., Garaniya, V., Abbassi, R., Jahangiri, S., Enshaei, H., Kam, U. S., Kimball, R.,
384 Yang, L., Zare, A., Bartlett, H., and Brown, R. J.: On-board measurements of particle and gaseous emissions from a large cargo vessel at
385 different operating conditions, Environmental Pollution, https://doi.org/10.1016/j.envpol.2017.11.008, 2017.
386 Cooper, D. A.: Exhaust emissions from high speed passenger ferries, Atmospheric Environment, 35, 4189-4200,
387 http://dx.doi.org/10.1016/S1352-2310(01)00192-3, 2001.
388 Cooper, D. A.: HCB, PCB, PCDD and PCDF emissions from ships, Atmospheric Environment, 39, 4901-4912,
389 http://dx.doi.org/10.1016/j.atmosenv.2005.04.037, 2005.
390 Corbett, J. J., and Farrell, A.: Mitigating air pollution impacts of passenger ferries, Transportation Research Part D: Transport and
391 Environment, 7, 197-211, http://dx.doi.org/10.1016/S1361-9209(01)00019-0, 2002.
392 Corbett, J. J., and Koehler, H. W.: Updated emissions from ocean shipping, Journal of Geophysical Research: Atmospheres, 108, 4650,
393 10.1029/2003JD003751, 2003.
394 Corbett, J. J., Winebrake, J. J., Green, E. H., Kasibhatla, P., Eyring, V., and Lauer, A.: Mortality from Ship Emissions: A Global Assessment,
395 Environmental Science & Technology, 41, 8512-8518, 10.1021/es071686z, 2007a.
396 Corbett, J. J., Winebrake, J. J., Green, E. H., Kasibhatla, P., Eyring, V., and Lauer, A.: Mortality from Ship Emissions: A Global Assessment,
397 Environmental Scinece & Technology, 41, 8512–8518, http://dx.doi.org/10.1021/es071686z, 2007b.
398 DJI S800-evo: http://www.dji.com/product/spreading-wings-s800-evo, 2014.
399 Eyring, V., Köhler, H. W., van Aardenne, J., and Lauer, A.: Emissions from international shipping: 1. The last 50 years, Journal of
400 Geophysical Research: Atmospheres, 110, D17305, 10.1029/2004JD005619, 2005.
401 Fierz, M., Burtscher, H., Steigmeier, P., and Kasper, M.: Field measurement of particle size and number concentration with the Diffusion
402 Size Classifier (DiSC), SAE Technical Paper, 2008.
403 Fuglestvedt, J., Berntsen, T., Eyring, V., Isaksen, I., Lee, D. S., and Sausen, R.: Shipping Emissions: From Cooling to Warming of Climate—
404 and Reducing Impacts on Health, Environmental Science & Technology, 43, 9057-9062, 10.1021/es901944r, 2009.
405 Gonzalez, F., Castro, M. P. G., Narayan, P., Walker, R., and Zeller, L.: Development of an autonomous unmanned aerial system to collect
406 time-stamped samples from the atmosphere and localize potential pathogen sources, Journal of Field Robotics, 28, 961-976,
407 10.1002/rob.20417, 2011.
408 Hak, C. S., Hallquist, M., Ljungström, E., Svane, M., and Pettersson, J. B. C.: A new approach to in-situ determination of roadside particle
409 emission factors of individual vehicles under conventional driving conditions, Atmospheric Environment, 43, 2481-2488,
410 http://dx.doi.org/10.1016/j.atmosenv.2009.01.041, 2009.
411 Hallquist, Å. M., Fridell, E., Westerlund, J., and Hallquist, M.: Onboard Measurements of Nanoparticles from a SCR-Equipped Marine
412 Diesel Engine, Enironmental Science & Technology, 47, 773-780, http://dx.doi.org/10.1021/es302712a, 2013a.
413 Hallquist, Å. M., Fridell, E., Westerlund, J., and Hallquist, M.: Onboard Measurements of Nanoparticles from a SCR-Equipped Marine
414 Diesel Engine, Environmental Science & Technology, 47, 773-780, 10.1021/es302712a, 2013b.
415 Hobbs, P. V., Garrett, T. J., Ferek, R. J., Strader, S. R., Hegg, D. A., Frick, G. M., Hoppel, W. A., Gasparovic, R. F., Russell, L. M., and
416 Johnson, D. W.: Emissions from ships with respect to their effects on clouds, Journal of the atmospheric sciences, 57, 2570-2590, 2000.
417 Inc., P.: Picarro G2401 Analyzer. 2017.
418 Isakson, J., Persson, T. A., and Selin Lindgren, E.: Identification and assessment of ship emissions and their effects in the harbour of
419 Göteborg, Sweden, Atmospheric Environment, 35, 3659-3666, http://dx.doi.org/10.1016/S1352-2310(00)00528-8, 2001.

Jayaratne, E. R., Ristovski, Z. D., Meyer, N., and Morawska, L.: Particle and gaseous emissions from compressed natural gas and ultralow sulphur diesel-fuelled buses at four steady engine loads, Science of The Total Environment, 407, 2845-2852, http://dx.doi.org/10.1016/j.scitotenv.2009.01.001, 2009.

Juwono, A. M., Johnson, G. R., Mazaheri, M., Morawska, L., Roux, F., and Kitchen, B.: Investigation of the airborne submicrometer particles emitted by dredging vessels using a plume capture method, Atmospheric Environment, 73, 112-123, http://dx.doi.org/10.1016/j.atmosenv.2013.03.024, 2013.

Kasper, A., Aufdenblatten, S., Forss, A., Mohr, M., and Burtscher, H.: Particulate Emissions from a Low-Speed Marine Diesel Engine, Aerosol Science and Technology, 41, 24-32, http://dx.doi.org/10.1080/02786820601055392, 2007.

Lack, D., Lerner, B., Granier, C., Baynard, T., Lovejoy, E., Massoli, P., Ravishankara, A. R., and Williams, E.: Light absorbing carbon emissions from commercial shipping, Geophysical Research Letters, 35, L13815, http://dx.doi.org/10.1029/2008GL033906, 2008.

Lack, D. A., Corbett, J. J., Onasch, T., Lerner, B., Massoli, P., Quinn, P. K., Bates, T. S., Covert, D. S., Coffman, D., Sierau, B., Herndon, S., Allan, J., Baynard, T., Lovejoy, E., Ravishankara, A. R., and Williams, E.: Particulate emissions from commercial shipping: Chemical, physical, and optical properties, Journal of Geophysical Research: Atmospheres, 114, D00F04, http://dx.doi.org/10.1029/2008JD011300, 2009.

Lack, D. A., Cappa, C. D., Langridge, J., Bahreini, R., Buffaloe, G., Brock, C., Cerully, K., Coffman, D., Hayden, K., Holloway, J., Lerner, B., Massoli, P., Li, S.-M., McLaren, R., Middlebrook, A. M., Moore, R., Nenes, A., Nuaaman, I., Onasch, T. B., Peischl, J., Perring, A., Quinn, P. K., Ryerson, T., Schwartz, J. P., Spackman, R., Wofsy, S. C., Worsnop, D., Xiang, B., and Williams, E.: Impact of Fuel Quality Regulation and Speed Reductions on Shipping Emissions: Implications for Climate and Air Quality, Environmental Science & Technology, 45, 9052-9060, 10.1021/es2013424, 2011.

Malaver Rojas, J. A., Gonzalez, L. F., Motta, N., Villa, T. F., Etse, V. K., and Puig, E.: Design and flight testing of an integrated solar powered UAV and WSN for greenhouse gas monitoring emissions in agricultural farms, International Conference on Intelligent Robots and Systems, Big Sky, Montana, USA, 2015 IEEE/RSJ, 2015, 1-6,

Mazaheri, M., Johnson, G. R., and Morawska, L.: Particle and Gaseous Emissions from Commercial Aircraft at Each Stage of the Landing and Takeoff Cycle, Environmental Science & Technology, 43, 441-446, 10.1021/es8013985, 2009.

Mueller, L., Jakobi, G., Czech, H., Stengel, B., Orasche, J., Arteaga-Salas, J. M., Karg, E., Elsasser, M., Sippula, O., Streibel, T., Slowik, J. G., Prevot, A. S. H., Jokiniemi, J., Rabe, R., Harndorf, H., Michalke, B., Schnelle-Kreis, J., and Zimmermann, R.: Characteristics and temporal evolution of particulate emissions from a ship diesel engine, Applied Energy, 155, 204-217, http://dx.doi.org/10.1016/j.apenergy.2015.05.115, 2015.

Murphy, S., Agrawal, H., Sorooshian, A., Padró, L. T., Gates, H., Hersey, S., Welch, W. A., Jung, H., Miller, J. W., Cocker Iii, D. R., Nenes, A., Jonsson, H. H., Flagan, R. C., and Seinfeld, J. H.: Comprehensive simultaneous shipboard and airborne characterization of exhaust from a modern container ship at sea, Environ. Sci. Technol., 43, 4626-4640, http://dx.doi.org/10.1021/es802413j, 2009.

Petzold, A., Hasselbach, J., Lauer, P., Baumann, R., Franke, K., Gurk, C., Schlager, H., and Weingartner, E.: Experimental studies on particle emissions from cruising ship, their characteristic properties, transformation and atmospheric lifetime in the marine boundary layer, Atmos. Chem. Phys., 8, 2387-2403, 10.1029/2004GL020312, 2008.

Petzold, A., Weingartner, E., Hasselbach, J., Lauer, P., Kurok, C., and Fleischer, F.: Physical properties, chemical composition, and cloud forming potential of particulate emissions from a marine diesel engine at various load conditions, Environ. Sci. Technol., 44, 3800-3805, http://dx.doi.org/10.1021/es903681z, 2010.

Pirjola, L., Pajunoja, A., Walden, J., Jalkanen, J. P., Rönkkö, T., Kousa, A., and Koskentalo, T.: Mobile measurements of ship emissions in two harbour areas in Finland, Atmospheric Measurement Techniques, 7, 149-161, http://dx.doi.org/10.5194/amt-7-149-2014, 2014.

Reda, A. A., Schnelle-Kreis, J., Orasche, J., Abbaszade, G., Lintelmann, J., Arteaga-Salas, J. M., Stengel, B., Rabe, R., Harndorf, H., Sippula, O., Streibel, T., and Zimmermann, R.: Gas phase carbonyl compounds in ship emissions: Differences between diesel fuel and heavy fuel oil operation, Atmospheric Environment, 112, 370-380, http://dx.doi.org/10.1016/j.atmosenv.2015.03.057, 2015.

Ristovski, Z. D., Miljevic, B., Surawski, N. C., Morawska, L., Fong, K. M., Goh, F., and Yang, I. A.: Respiratory health effects of diesel particulate matter, Respirology, 17, 201-212, http://dx.doi.org/10.1111/j.1440-1843.2011.02109.x, 2012.

Schreier, S. F., Peters, E., Richter, A., Lampel, J., Wittrock, F., and Burrows, J. P.: Ship-based MAX-DOAS measurements of tropospheric NO_2 and SO_2 in the South China and Sulu Sea, Atmospheric Environment, 102, 331-343, http://dx.doi.org/10.1016/j.atmosenv.2014.12.015, 2015.

Sinha, P., Hobbs, P. V., Yokelson, R. J., Christian, T. J., Kirchstetter, T. W., and Bruintjes, R.: Emissions of trace gases and particles from two ships in the southern Atlantic Ocean, Atmospheric Environment, 37, 2139-2148, http://dx.doi.org/10.1016/S1352-2310(03)00080-3, 2003.

Streets, D. G., Carmichael, G. R., and Arndt, R. L.: Sulfur dioxide emissions and sulfur deposition from international shipping in Asian waters, Atmospheric Environment, 31, 1573-1582, http://dx.doi.org/10.1016/S1352-2310(96)00204-X, 1997.

UNCTAD: Review of Maritime Transport 2015, United Nations Conference on Trade and Development UNCTAD, 2015.

USEPA-OTAC: USEPA-OTAC, 2012. http://www.epa.gov/otaq/oceanvessels.htm#regs, Ocean Vessels and Large Ships. US Environmental Protection Agency, Office-of-Transportation-and-Air-Quality. , 2012.

Viana, M., Hammingh, P., Colette, A., Querol, X., Degraeuwe, B., Vlieger, I. d., and Van Aardenne, J.: Impact of maritime transport emissions on coastal air quality in Europe, Atmospheric Environment, 90, 96-105, http://dx.doi.org/10.1016/j.atmosenv.2014.03.046, 2014.

Westerlund, J., Hallquist, M., and Hallquist, Å. M.: Characterization of fleet emissions from ships through multi-individual determination of size-resolved particle emissions in a coastal area, Atmospheric Environment, 112, 159-166, http://dx.doi.org/10.1016/j.atmosenv.2015.04.018, 2015.

WHO: Review of evidence on health aspects of air pollution 2013.

Williams, E. J., Lerner, B. M., Murphy, P. C., Herndon, S. C., and Zahniser, M. S.: Emissions of NOx, SO2, CO, and HCHO from commercial marine shipping during Texas Air Quality Study (TexAQS) 2006, Journal of Geophysical Research: Atmospheres, 114, D21306, 10.1029/2009JD012094, 2009.

Winnes, H., Moldanová, J., Anderson, M., and Fridell, E.: On-board measurements of particle emissions from marine engines using fuels with different sulphur content, Proc. Inst. Mech. Eng. Part M J. Eng. Marit. Environ., 230, 45-54, 10.1177/1475090214530877, 2016.

486